

Article

Distribution and Environmental Impact of Expanded Polystyrene Buoys from Korean Aquaculture Farms

Seongbong Seo  and Young-Gyu Park * 

Ocean Circulation and Climate Research Department, Korea Institute of Ocean Science and Technology, Busan 49111, Republic of Korea; sbseo@kiost.ac.kr

* Correspondence: ypark@kiost.ac.kr

Abstract: Expanded polystyrene (EPS) buoys, commonly employed in South Korean aquaculture farms, are prone to fragmentation, generating substantial marine debris. The trajectories of EPS buoys dislocated from aquaculture farms were investigated using a Lagrangian particle-tracking model. Daily ocean current data from the 1/12° Hybrid Coordinate Ocean Model analysis and wind data from the 1/4° European Center for Medium-Range Weather Forecasts reanalysis were used as inputs. The particles were released daily, and the initial positions and number of particles were determined based on the usage of EPS buoys. Because EPS buoys are highly buoyant, both wind and ocean currents considerably influence their movement. To account for variations in the buoyancy of these buoys, three experiments were conducted, each considering different levels of windage. The simulation results closely aligned with the observed coastal distribution patterns of the large EPS debris. As the windage increases, the particles exhibit a swifter deviation from their original locations, highlighting the need for effective local management. Moreover, this increased windage affects the distribution patterns in regional seas, reducing the number of particles that flow into the East Sea, while increasing the number of particles that migrate into the Yellow Sea and East China Sea.

Keywords: plastic debris; EPS buoy; coastal accumulation; Lagrangian particle-tracking model



Citation: Seo, S.; Park, Y.-G.

Distribution and Environmental Impact of Expanded Polystyrene Buoys from Korean Aquaculture Farms. *J. Mar. Sci. Eng.* **2024**, *12*, 256. <https://doi.org/10.3390/jmse12020256>

Academic Editor: Chengjun Sun

Received: 3 January 2024

Revised: 27 January 2024

Accepted: 30 January 2024

Published: 31 January 2024



Copyright: © 2024 by the authors. Licensee MDPI, Basel, Switzerland. This article is an open access article distributed under the terms and conditions of the Creative Commons Attribution (CC BY) license (<https://creativecommons.org/licenses/by/4.0/>).

1. Introduction

Expanded polystyrene (EPS, commonly known as Styrofoam) is an inexpensive, readily processed, and highly buoyant material, rendering it suitable for diverse applications. In South Korea, particularly along the southern coast, EPS-based buoys are commonly used in aquaculture farms in the cultivation of seaweeds, abalone, fish, oysters, mussels, and sea squirts (Figure 1). As of 2017, approximately 52 million EPS buoys are deployed annually in domestic coastal regions [1]. Notably, sea mustard (30%), laver (29%), and oyster farms (18%) collectively account for about 77% of the total buoy usage, and with the inclusion of kelp (10%) and abalone (9%), they comprise approximately 96%.

Despite their utility, EPS buoys have emerged as a major source of marine debris along the South Korean coast. By 2021, plastics comprised over 80% of the country's total coastal debris, with EPS contributing to over 20% of plastic waste [2]. Although the South Korean government imposed a ban on new EPS buoys in November 2022, challenges remain in managing existing buoys and adopting eco-friendly alternatives. These drifting buoys not only pose economic threats to marine ecosystems and the tourism sector [3] but are also fragmented into smaller-sized microplastics through physical, chemical, and biological processes [4]. EPS microplastics are frequently reported along the South Korean coast [5,6]. In particular, Lee et al. [7] assessed the generation of debris in the Gyeongsangnam-do province by examining the usage, annual input, loss, recovery, and illegal disposal rates of EPS buoys; they revealed that the annual debris generation rate is approximately 11% of the total usage. However, limited information is available on the movement of EPS buoys and their impact on various locations once they disengage from aquaculture farms.

Considering these aspects, characterizing the pathways of EPS buoys originating from aquaculture farms is essential to effectively mitigate their environmental impacts.

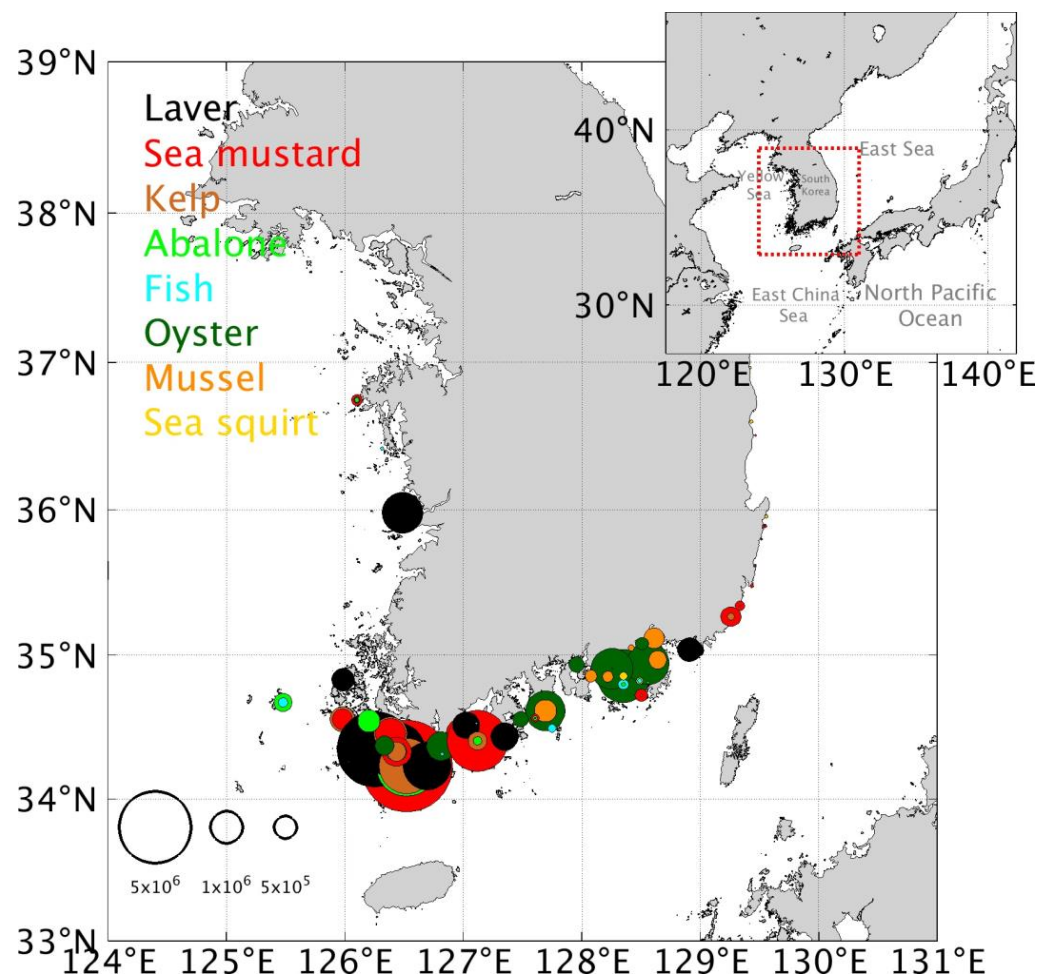


Figure 1. Locations of aquaculture farms along the coast of South Korea and corresponding usage of EPS buoys.

Particle-tracking models are valuable tools for tracing floating marine debris. Previous studies have indicated that windage, in combination with ocean currents, significantly shapes the movement of floating debris [8–14]. Maximenko et al. [9] and Murray et al. [10] demonstrated that items with high windage, such as EPS and buoys, traversed the Pacific Ocean to reach the Canadian coast more swiftly than items with low windage in the aftermath of the 2011 earthquake-induced tsunami. Yoon et al. [14] used a model to simulate the distribution of plastic waste in the East Sea by considering five levels of buoyancy. To account for windage, they varied the ratio of the plastic exposed to air and submerged in water between 0 and 100%, with the corresponding windage ranging from 0 to 30%, revealing that the residence time of plastics in the East Sea strongly depended on windage. Additionally, Seo and Park [11] used windages between 0 and 5% to model buoyant plastic debris discharged from rivers entering the seas around the Korean Peninsula. They demonstrated that windage significantly influenced the rate at which plastic debris reached the Northwestern Pacific coast. In particular, previous studies have primarily focused only on tracking plastic debris stemming from accidents or population sources and have not explored the movement of EPS buoys originating from aquaculture sites.

To address this research gap, this study investigates the movement characteristics and arrival of EPS floats originating from aquaculture farms on the southern coast of South Korea (Figure 2) using a Lagrangian particle-tracking model. Our aim is to comprehend

transboundary transport and beaching by analyzing the dispersal of these particles in the Northwestern Pacific waters around the Korean Peninsula. We intend to compare the movements of buoys used in aquaculture farms by applying varying levels of windage, while also considering the conditions of the buoys in use. Section 2 presents details on the model and experimental conditions. Moreover, we validated the model outcomes by comparing them with coastal observation data, and the corresponding results along with a discussion on the limitations of the model are presented in Section 3. Finally, Section 4 concludes this paper, summarizing this study and the implications of the findings.



Figure 2. (a) EPS buoy floating near aquaculture farms, (b) fragmented and weathered EPS buoy and plastic debris reaching coastal shore.

2. Materials and Methods

2.1. Buoy-Tracking Model

The model used in this study is based on the following equation, as described in previous studies by Seo and Park [11,12] and Seo et al. [13]:

$$\vec{x}_{t+\Delta t} = \vec{x}_t + \int_t^{t+\Delta t} \left\{ \vec{u}_c(\vec{x}_t, \tau) + W_f \times \vec{w}_{10m}(\vec{x}_t, \tau) \right\} d\tau + R\sqrt{2K_h\Delta t} \quad (1)$$

where \vec{x}_t represents the geographical position of a particle at time t , and Δt denotes the time interval (1 h). For time integration, the Runge–Kutta 4th order method [15] is used. \vec{u}_c and \vec{w}_{10m} indicate the surface ocean current and wind at 10 m above sea level, respectively. $W_f \times \vec{w}_{10m}$ is the wind drift, where W_f is the windage coefficient. The windage coefficient is determined by the ratio between the amount of exposed to *Air* and submerged portions (*water*) of the EPS buoy ($W_f = 0.03 \times (\frac{Air}{water})^{\frac{1}{2}}$). The commonly used 60 L EPS buoys in coastal aquaculture farms have a density of 20 kg/m³, weighing approximately 2 kg, with a submerged volume of approximately 0.002 m³. In the unattached state, the ratio of the portion of the EPS buoy exposed to air to the portion submerged in water (*Air/water*) is approximately 27.35. Therefore, the maximum windage exhibited by EPS buoys is approximately 15%, which falls within the range of windages for plastic waste reported by Yoon et al. [14]. The term $R\sqrt{2K_h\Delta t}$ serves as a random walk component to simulate unresolved processes and sub-grid-scale turbulent motion [16]. Herein, R is a random number between -1 and 1 , and K_h is a horizontal diffusion coefficient based on the Smagorinsky [17] mixing scheme [11,13,18].

Buoyant EPS buoys can also reach and accumulate along the coast [11]. The coast is set based on a grid structure of input data. The grids with valid current data are treated as ocean, and the grids without current data are land, and the boundary between the land grids and ocean grids are treated as coastlines. Particles transported toward land grids are considered to have reached the coast, and resuspension is not considered.

2.2. Input Data

Three hourly surface currents obtained from the 1/12° HYbrid Coordinate Ocean Model (HYCOM, GOFS 3.1, <https://www.hycom.org/>, accessed on 29 January 2024) were used as input data. HYCOM assimilates a wide range of observational data such as satellite imagery, surface temperature, and ARGO float data to yield an accurate simulation of oceanic conditions. Notably, HYCOM successfully captured primary oceanic flows in the sea regions around the Korean peninsula, as illustrated in Figure 3. Within the study area, the Kuroshio Current is the most significant flow feature, as represented by the red arrows on the map. The Tsushima Warm Current originates from the Kuroshio Current in the East China Sea and flows eastward through the strait between southeastern Korea and Japan. Notably, the HYCOM does not incorporate tidal currents. The mean current strength in the study area ranges from 0.1 to 0.25 m/s, while the strength of the tidal current reaches up to about 1 m/s [19]. Thus, to account for short-term variability, tidal current data from the Oregon State University TOPEX/Poseidon Global Inverse Solution tidal model (OSU TPXO) [20] data were integrated with HYCOM ocean currents.

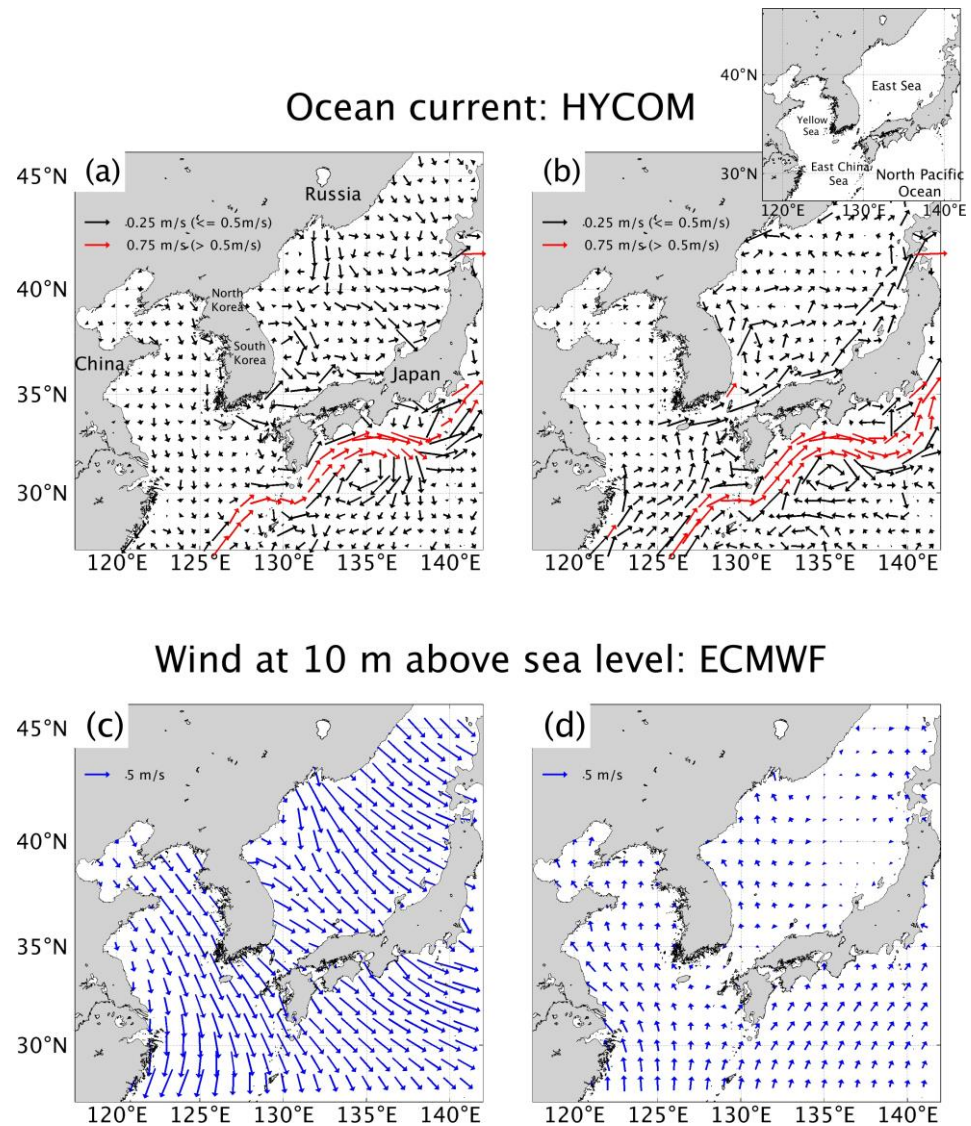


Figure 3. Mean surface velocity over the Northwest Pacific from the HYCOM GOFS 3.1 analysis for (a) winter and (b) summer from 2015 to 2017. Flows below 0.5 m/s are indicated by black arrows and flows above 0.5 m/s are indicated by red arrows. Mean wind at 10 m above sea level as obtained from ECMWF ERA5 in (c) winter and (d) summer for the same periods of ocean current.

For the wind data (\vec{w}_{10m}), we employed the 1/4° European Center for Medium-Range Weather Forecasts (ECMWF, <https://www.ecmwf.int/>, accessed on 29 January 2024) Reanalysis v5 (ERA5) at 3 h intervals. The wind patterns in the region exhibit distinct seasonality (Figure 3). Northwesterly winds prevail during winter, influenced by the Siberian high-pressure system, whereas southerly winds are dominant from spring to summer [21]. Based on ERA5 data, the seasonal average wind strength along the South Sea coast, where aquaculture farms are mainly located, is significantly stronger in winter, about 4.7 m/s, than in summer, about 1.1 m/s.

2.3. Experiments

Three types of plastic debris were considered as illustrated in Figure 4. Type A is an EPS buoy with a maximum windage of approximately 15% owing to its buoyancy. Type B is also an EPS buoy but is assumed to be weighed down by attached marine organisms or ropes (Figure 2a), resulting in greater submersion in seawater. Assuming that 75% of the buoy section is exposed to air and approximately 25% is submerged, the ratio of the buoy section exposed to air and water is approximately 4.04, with a windage of approximately 6%. Finally, Type C is a neutrally buoyant plastic, such as small plastic fragments, that is not exposed to air and is therefore unaffected by wind.

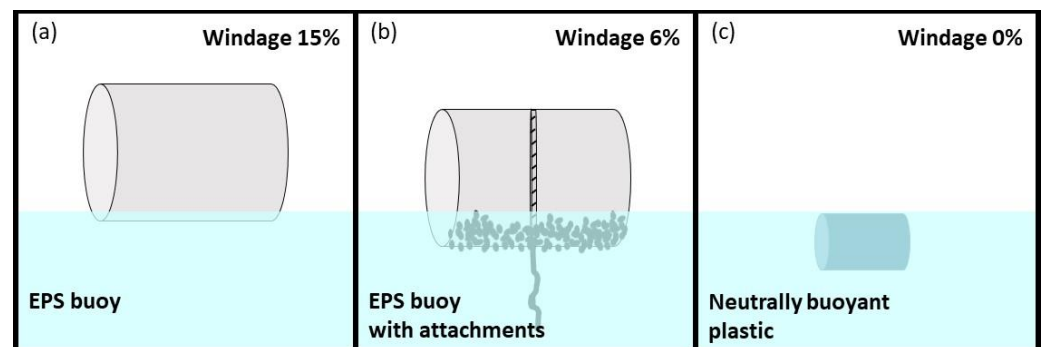


Figure 4. Types of EPS buoy and windage: (a) EPS buoy with 15% windage for Type A, (b) EPS buoy with attachments with 6% windage for Type B, (c) and neutrally buoyant plastic without windage for Type C.

The locations and amounts of particles released were determined based on the usage of buoys at individual aquaculture sites, as shown in Figure 1. The top 30 aquaculture sites were selected as the release points. We assumed that approximately 10% of buoys are dislocated in the ocean [7]. From these 30 locations, a consistent number of particles, ranging from 1 to 36, based on the actual usage at each farm, were released daily for each aquaculture site from 2015 to 2017, and the trajectories of these particles were traced for a duration of one year. The selected 30 sites accounted for approximately 94% of the total buoy usage as shown in Figure 1. Approximately 75,000 particles were released for each windage experiment, resulting in 225,000 particles across three experiments.

2.4. Probability Function

The experimental results were analyzed using the probability function reported by Rypina et al. [22], which illustrates the main pathway of particles, similar to the work of Seo and Park [11]. The study area was gridded into a $0.5^\circ \times 0.5^\circ$ square, and the probability (P_{ij}) of reaching each grid point (i, j) from the aquaculture farms was estimated as follows:

$$P_{i,j} = \frac{N_{ij}}{N_{total}} \quad (2)$$

where i indicates the zonal direction, j represents the meridional direction, N_{ij} denotes the number of particles reaching each grid, and N_{total} depicts the total number of particles.

In each experiment, it is necessary to exclude the impact of particles originating from aquaculture sites that reach the coast soon after their release. Therefore, particles that reached the coast within 3 days after release were excluded from the probability calculation. The numbers of particles (N_{total}) used in the calculations for Types A, B, and C were about 71,300, 79,300, and 127,500, respectively.

3. Result and Discussion

3.1. Pathways

Figure 5 illustrates the trajectories of the three types of floating objects over the course of one year. Type A was primarily influenced by wind and predominantly drifted within the East China Sea and the Yellow Sea, with limited occurrences in the East Sea or the northwestern Pacific. In contrast, Type B was distributed across the entire research area, except for the northern Yellow Sea, and Type C predominantly occurred in the East Sea and remained around its release point. In particular, these particles were infrequent in the northern Yellow Sea and near the Pacific Ocean. Simulations conducted over two and three years exhibited similar characteristics.

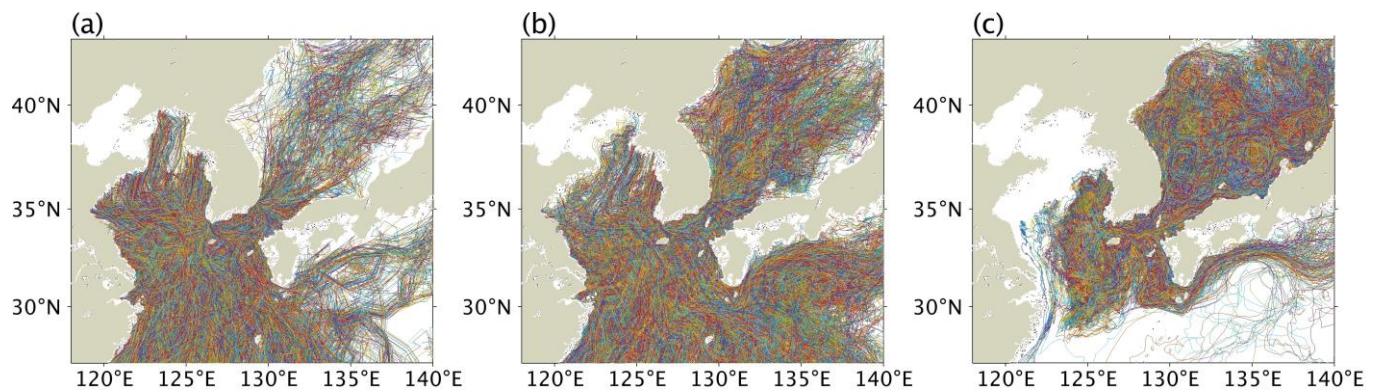


Figure 5. Particle trajectories obtained via EPS buoy-tracking experiment: (a) EPS buoy with 15% windage for Type A, (b) EPS buoy with attachments with 6% windage for Type B, (c) and neutrally buoyant plastic without windage for Type C. Colors represent individual trajectories.

To further assess the average distribution patterns, the study area was divided into $0.5^\circ \times 0.5^\circ$ grid cells, and the probability distributions were evaluated, as depicted in Figure 6. The areas with higher probabilities indicate the main particle paths. Generally, the probabilities decrease with distance from the origin. Notably, higher windage led to decreased probabilities within offshore grids near the coastal release point, implying that wind facilitated the efficient escape of particles from the coastal area.

In the waters surrounding the Korean Peninsula, including the South Sea where aquaculture farms are located, northwesterly winds dominate in the winter, while southeasterly winds prevail in the summer. These seasonal wind patterns significantly influence particle movement, with southeasterly winds during summer driving particles toward the coast, whereas northwesterly winds during winter tend to push offshore particles toward the southern region of the East China Sea. The probability distributions for Type A and Type B particles are mainly toward the southern East China Sea. From autumn to winter, when northerly winds become stronger, particles disperse southwards as shown in the mean probability distributions. On the other hand, in summer, when southerly winds are active, dispersion along the western coast of South Korea is dominant, especially for Type A, which is affected by wind more. For Type C, with 0% windages, the pathways were primarily determined by the Jeju Warm Current and the Tsushima Warm Current. These particles generally followed a course through the Korea Strait into the East Sea, consistent with the findings of Seo and Park [11] regarding particles originating from a river on the southern coast of the Korean Peninsula. After flowing into the East Sea, the particles move eastward

along the East Korea Warm Current and Nearshore branch and are mainly distributed in the southern part of the East Sea.

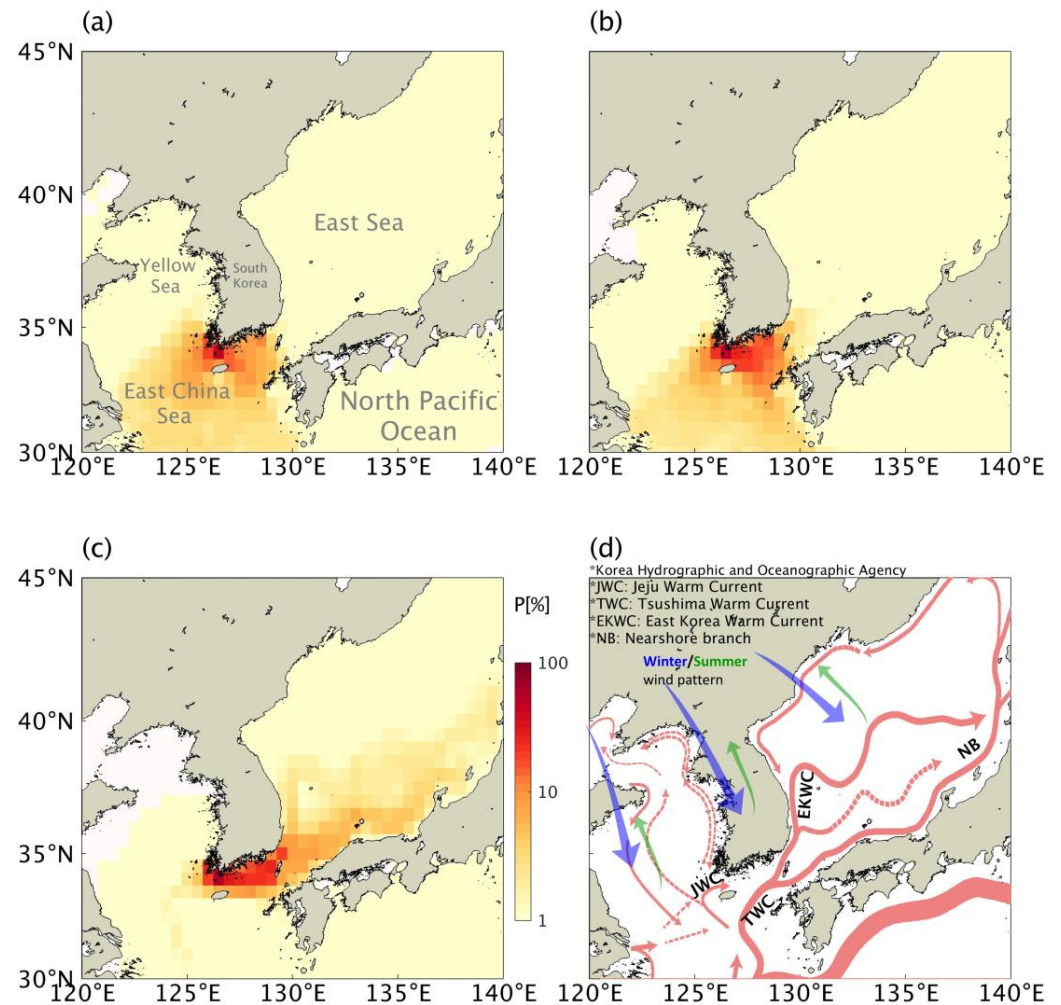


Figure 6. Mean probability distribution of EPS buoy particles originating from aquaculture farms of (a) EPS buoy with 15% windage for Type A, (b) EPS buoy with attachments and 6% windage for Type B, (c) neutrally buoyant plastic without windage for Type C. (d) Schematic diagram of ocean currents (red arrows) around the Korean peninsula from the Korea Hydrographic and Oceanographic Agency (KHOA) and seasonal wind patterns (blue and green arrows).

3.2. Coastal Accumulation on the Coast of South Korea: Comparison with Observations

The number of particles arriving at the coast was compared with the observed data in Figure 7. Observational data were obtained from the Marine Environment Information System (<https://www.meis.go.kr>, accessed on 29 January 2024), reported by the Ministry of Oceans and Fisheries of Korea. These data covered the average distribution of EPS buoys (measuring 50 cm or larger) over a 10-year span from 2008 to 2017 along the South Korean coast at 20 different locations. These data were obtained by civilian volunteers at each point along a 100 m length of coastline, and we compared the main trends with the distribution results of our model simulations.

The simulation results were compared with the observations at the same 20 locations, as illustrated in Figure 7. All three simulations showed the highest particle densities at L11 and L12, on the southern coast of South Korea, where most aquaculture farms are located and where EPS buoy usage is highest (Figure 7a–c). Similar to the simulations, the observations also showed the highest EPS buoy distribution at L12 on the southwestern coast, with more than 26 items per 100 m (Figure 7d).

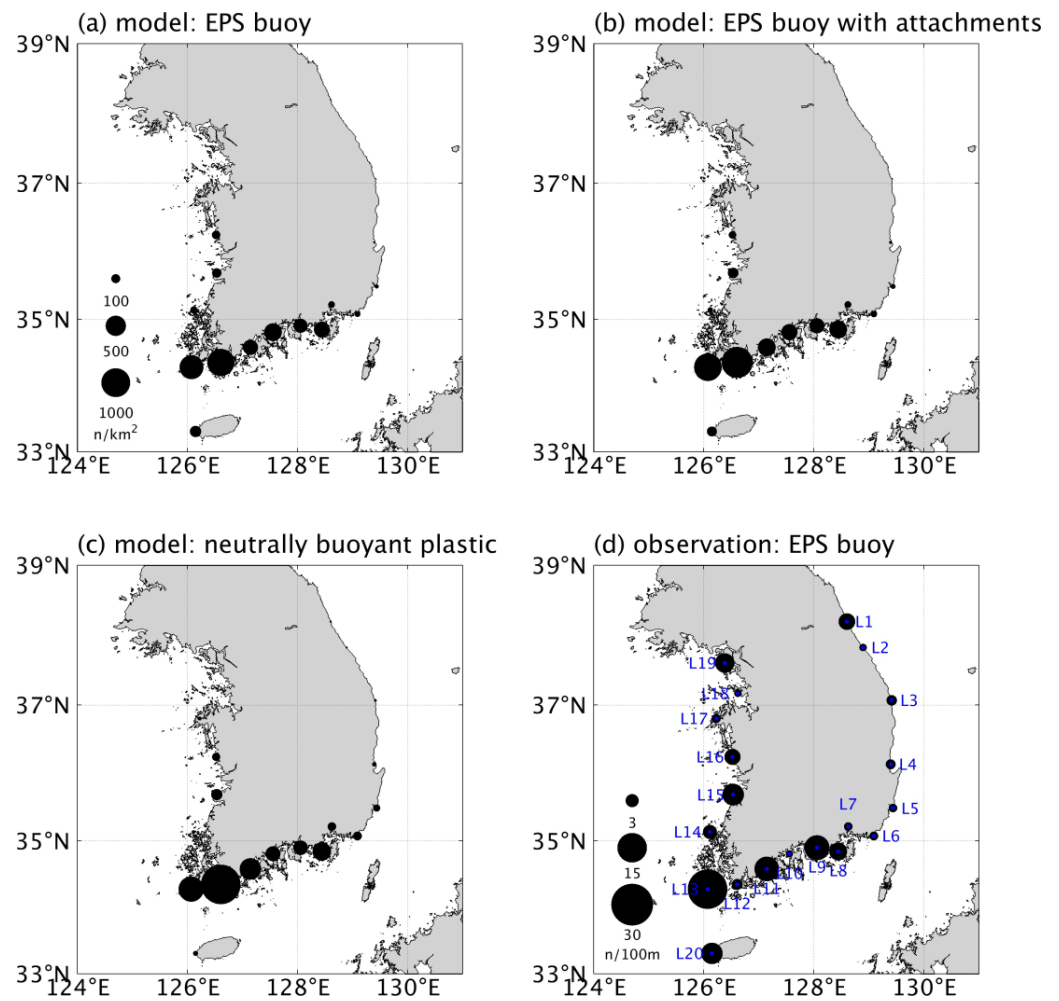


Figure 7. The amount of modeled EPS buoys at 20 locations: (a) 15% windage for Type A, (b) 6% windage for Type B, (c) 0% windage for Type C. (d) Ten-year average concentration distribution (2008–2017) of EPS buoys larger than 50 cm at 20 coastal locations from the Marine Environment Information System of Korea (<https://www.meis.go.kr/>, accessed on 29 January 2024).

To compare the spatial distribution of model data with the variability of observational data, correlation coefficients were used. The correlation coefficients for the simulation results of Types A, B, and C compared to the observations were 0.49, 0.52, and 0.27, respectively. The variance linked to windage is apparent, and the simulation aligns most closely with the observations when a more realistic windage, as seen in Type B, is considered. However, notable discrepancies existed, especially in the far northern areas of the western (L19) and eastern (L1) coasts, where the observed counts exceeded five items per 100 m. This discrepancy can be attributed to the model primarily concentrating on particle emissions from the southern coast of South Korea, suggesting that prevailing currents and winds make it unlikely for particles to reach the farthest northern regions of the western and southern coasts. It is plausible that the EPS buoys observed in these areas do not originate from southern aquaculture farms, but from other sources such as harbors, ships, or fishing markers. Another possibility is that the northernmost part of the west coast of South Korea is of foreign origin. Floating plastic debris released from estuaries of Chinese rivers like the Yangtze and Yellow Rivers can change their paths depending on windage [11]. Specifically, floating plastic debris from the Yangtze River, in the absence of windage, tends to spread through the East China Sea to the southern coast of South Korea and the southern part of the East Sea. However, with an increase in windage up to 5%, the trajectory can shift toward the north, into the Yellow Sea. Consequently, this could potentially lead the debris

to reach the western coast of South Korea, adjacent to the Yellow Sea. A similar pattern might be observed for EPS buoys that were lost near the Chinese coast. Therefore, it is possible that EPS buoys from aquaculture farms near Shandong, Jiangsu, and Zhejiang on the Chinese coast [23] or on the coast of Taiwan [24] could end up on the western coast of South Korea.

3.3. Destination

In a three-year simulation, the distribution of Types A, B, and C was assessed across 10 different coastal regions around the Korean Peninsula [11]. Of these regions, eight are coastlines, including three along the Korean Peninsula, and the others are in Japan, China, and Russia, as well as the major islands of Jeju and Tsushima. The particles leaving the study area toward the open ocean through the southern and eastern boundaries (Figure 8) were also counted.

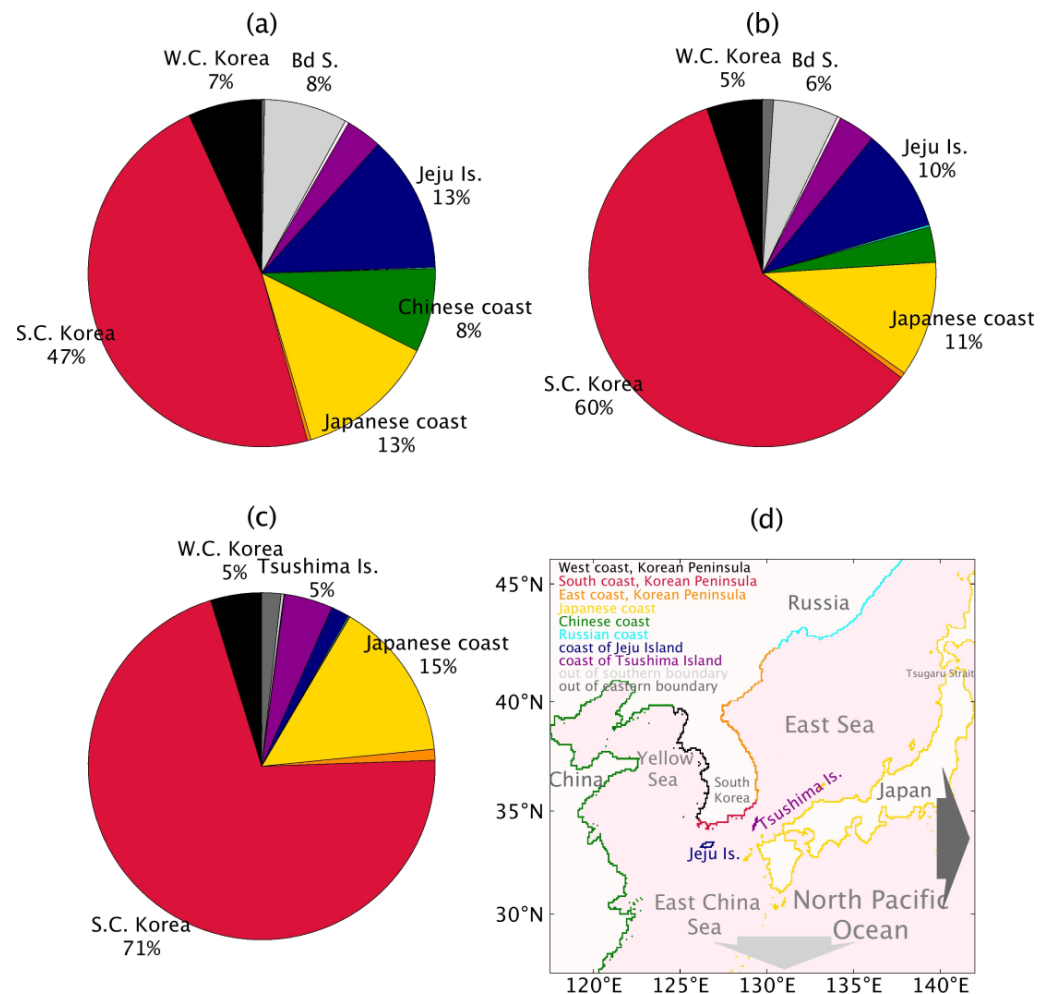


Figure 8. Coastal arrival ratio for EPS buoy-tracking experiments, (a) EPS buoy with 15% windage for Type A, (b) EPS buoy with attachments and 6% windage for Type B, (c) neutrally buoyant plastic without windage for Type C. Only arrivals of 5% or more are shown with name of coastal area. (d) Classification of the coastal areas and the destination of the EPS buoy particles.

Across all three experiments, the southern coast of South Korea, the initial release point for particles, consistently displayed the most significant concentration, as illustrated in Figure 8. This aligns with earlier studies that focused on pollutants or debris emanating from rivers [11,25]. The percentage of particles near the point of coastal release varied between types, with as low as 47% for Type A and as high as 71% for Type C. The stronger

the wind effect, the more likely particles were to travel further away from their release point, thereby enhancing their impact on other shores.

Regarding particles reaching other coastlines, Type A constituted the majority of particles found along the coasts of Jeju Island and China. Conversely, on the Japanese coast, Type C accounted for the majority (15%). The proportions of Types A and B were 13% and 11%, respectively. This variation can be attributed to the different oceanic pathways influenced by the two types. Types A and B primarily affected the western coast of Japan by wind, whereas Type C was largely influenced by the Tsushima Warm Current and Nearshore branch and tended to impact the northern coast of Japan. The results of this study are comparable to those of Seo and Park [12], which accounted for windages ranging from 0 to 4%. Their research across the North Pacific demonstrated that with 0 to 2% windage, particles could potentially reach the Great Pacific Garbage Patch in the Eastern Pacific. In our study, about 2% of particles in Type C crossed the eastern boundary into the Pacific, which is a higher rate compared to Type A and B. Additionally, at 4% windage, floating debris could cross the southern boundary of our study area, potentially impacting areas like Taiwan or the Philippine Sea and coastlines. In the results for Type A and B, 8% and 6% of particles, respectively, were transported across the southern boundary. These EPS buoys with higher windages have the potential to reach areas like Taiwan or the Philippine Sea, similar to the findings of Seo and Park [12]. Such scenarios can lead to transboundary transport, and depending on the case, might influence the potential spread of invasive species due to the transportation of marine organisms attached to the floating debris [26,27].

4. Conclusions

In this study, we employed a Lagrangian particle-tracking model to investigate the movement of EPS buoys commonly used in aquaculture farms in Korea. To account for variations in the buoyancy of these buoys, three experiments were conducted, each considering different levels of windage on the state of the buoys: maximum windage at 15% for the EPS buoy without any attachments, moderate windage at 6% for the EPS buoy with attachments, and no windage for submerged plastic debris such as small plastic fragments. The research results demonstrated a strong dependence of particle trajectories, average paths, and coastal arrivals on windage or buoyance.

The probability decreased monotonically away from the origin, suggesting a lack of convergence zones within our study area as in Seo and Park [11]. The majority of the particles reached the shoreline near their point of origin, in line with the model predictions and actual observations. At 0% windage, the particles flowed into the East Sea from the South Sea. As the windage increased, more particles escaped to the East China Sea and the Yellow Sea. Additionally, due to the stronger windage, EPS buoys were more likely to drift from the Chinese coast into the open seas of the Pacific Ocean when compared to submerged plastic ones. These findings underscore that even when originating from the same origin, the buoyancy of plastics can dictate their movement patterns and final destinations. Consequently, the proportion of particles crossing boundaries has increased, emphasizing the need for meticulous management of floating debris.

The model results show wind-driven dispersal from the south coast of Korea, where the aquaculture farms are located, as seen in the mean probability distribution. In the winter, northwesterly winds contribute to a more pronounced offshore displacement of particles, while in the summer, southeasterly winds tend to push them toward the coast. Considering that production at these aquaculture farms mainly occurs in the winter months, there is a need to consider seasonality in the management of coastal debris.

The transboundary transport of particles, as highlighted in Section 3.3, raises a significant ecological concern regarding the potential spread of invasive species [26]. EPS buoys or plastics can act as vehicles for various coastal organisms, facilitating their transport across vast oceanic distances to new environments where they could become invasive [27]. Invasive species, once introduced to non-native ecosystems, can disrupt local biodiver-

sity, alter habitat structures, and even impact local economies, particularly in coastal and marine communities, so they require attention through continuous monitoring in areas of potential impact.

Our model results show overall patterns of EPS buoy accumulation. Although the beaching of floating debris is a complex process [28,29], we have used a rather simplified beaching parametrization. Furthermore, the resolution of the ocean model is not high enough to fully represent the coastline of the South Sea of the Korean Peninsula. Therefore, to make a more localized assessment, it is necessary to use higher-resolution model outputs along with improved beaching parameterization considering shoreline types and tidal ranges [30].

Further research is imperative to comprehensively understand the flow of EPS buoy debris into the Pacific Ocean and its accumulation in marine environments. A previous study by Seo and Park [12] demonstrated that buoys from the southern coast of Jeju could enter the Pacific Ocean through the East China Sea. These buoys could have reached the North Pacific and U.S. coasts over a span of five years under a windage of approximately 2%. In contrast, EPS type buoys, as considered in our study, are less robust and more susceptible to deformation compared to the coastal wave buoys tracked by Seo and Park [12], which maintain stability without deformation for several years, even in marine environments. Moreover, EPS is likely to sink more quickly if it fragments from EPS buoys, potentially due to biological factors [31]. Considering these aspects, to effectively track the long-term behavior of EPS buoys entering the ocean, future research models should consider not only strong windage but also fragmentation and vertical movement induced by biofouling.

Author Contributions: Conceptualization, S.S. and Y.-G.P.; methodology, Y.-G.P.; software, S.S.; validation, S.S.; formal analysis, S.S. and Y.-G.P.; investigation, S.S.; resources, S.S.; data curation, S.S.; writing—original draft preparation, S.S.; writing—review and editing, Y.-G.P.; visualization, S.S.; supervision, Y.-G.P.; project administration, Y.-G.P.; funding acquisition, Y.-G.P. All authors have read and agreed to the published version of the manuscript.

Funding: This research was a grant from “Development of a global marine radioactive contamination effect prediction system (RS-2023-00256141)” and “Land/Sea-based input and fate of microplastics in the marine environment (20220357)” supported by the Korea Institute of Marine Science & Technology Promotion (KIMST) funded by the Ministry of Oceans and Fisheries.

Institutional Review Board Statement: Not applicable.

Informed Consent Statement: Not applicable.

Data Availability Statement: Data are contained within the article.

Acknowledgments: We are grateful to the editor and anonymous reviewers for their constructive comments.

Conflicts of Interest: The authors declare no conflicts of interest.

References

1. MOF. *Establishment of Integrated Management System for Waste Aquaculture Styrofoam Buoy*; MOF: Sejong-si, Republic of Korea, 2018. (In Korean)
2. KOEM. *National Coastal Litter Monitoring*; KOEM: Seoul, Republic of Korea, 2021. (In Korean)
3. Jang, S.W.; Kim, D.H.; Seong, K.T.; Chung, Y.H.; Yoon, H.J. Analysis of floating debris behaviour in the Nakdong River basin of the southern Korean peninsula using satellite location tracking buoys. *Mar. Pollut. Bull.* **2014**, *88*, 275–283. [[CrossRef](#)]
4. Song, Y.K.; Hong, S.H.; Eo, S.; Shim, W.J. The fragmentation of Nano-and microplastic particles from thermoplastics accelerated by simulated-sunlight-mediated photooxidation. *Environ. Pollut.* **2022**, *311*, 119847. [[CrossRef](#)]
5. Eo, S.; Hong, S.H.; Song, Y.K.; Lee, J.; Lee, J.; Shim, W.J. Abundance, composition, and distribution of microplastics larger than 20 μm in sand beaches of South Korea. *Environ. Pollut.* **2018**, *238*, 894–902. [[CrossRef](#)]
6. Hong, S.; Lee, J.; Kang, D.; Choi, H.W.; Ko, S.H. Quantities, composition, and sources of beach debris in Korea from the results of nationwide monitoring. *Mar. Pollut. Bull.* **2014**, *84*, 27–34. [[CrossRef](#)] [[PubMed](#)]
7. Lee, J.; Jang, Y.C.; Hong, S.Y.; Lee, J.S.; Kim, K.S.; Choi, H.J.; Hong, S. A study on the annual inflow and its control of Styrofoam buoy debris in oyster aquaculture farm in Gyeongnam, Korea. *Ocean Policy Res.* **2016**, *31*, 55–79.

8. Iskandar, M.R.; Park, Y.G.; Kim, K.; Jin, H.; Seo, S.; Kim, Y.H. Tracking the pumice rafts from the Fukutoku-Okanoba submarine volcano with Satellites and a Lagrangian Particles trajectory model. *Mar. Pollut. Bull.* **2023**, *193*, 115254. [[CrossRef](#)]
9. Maximenko, N.; Hafner, J.; Kamachi, M.; MacFadyen, A. Numerical simulations of debris drift from the Great Japan Tsunami of 2011 and their verification with observational reports. *Mar. Pollut. Bull.* **2018**, *132*, 5–25. [[CrossRef](#)]
10. Murray, C.C.; Maximenko, N.; Lippiatt, S. The influx of marine debris from the Great Japan Tsunami of 2011 to North American shorelines. *Mar. Pollut. Bull.* **2018**, *132*, 26–32. [[CrossRef](#)]
11. Seo, S.; Park, Y.G. Destination of floating plastic debris released from ten major rivers around the Korean Peninsula. *Environ. Int.* **2020**, *138*, 105655. [[CrossRef](#)]
12. Seo, S.; Park, Y.G. Tracking a coastal wave buoy, lost from the southern coast of Jeju Island, using Lagrangian particle modeling. *J. Mar. Sci. Eng.* **2021**, *9*, 795. [[CrossRef](#)]
13. Seo, S.; Park, Y.G.; Kim, K. Tracking flood debris using satellite-derived ocean color and particle-tracking modeling. *Mar. Pollut. Bull.* **2020**, *161*, 111828. [[CrossRef](#)]
14. Yoon, J.H.; Kawano, S.; Igawa, S. Modeling of marine litter drift and beaching in the Japan Sea. *Mar. Pollut. Bull.* **2010**, *60*, 448–463. [[CrossRef](#)]
15. Dormand, J.R.; Prince, P.J. A family of embedded Runge-Kutta formulae. *J. Comput. Appl. Math.* **1980**, *6*, 19–26. [[CrossRef](#)]
16. North, E.W.; Hood, R.R.; Chao, S.Y.; Sanford, L.P. Using a random displacement model to simulate turbulent particle motion in a baroclinic frontal zone: A new implementation scheme and model performance tests. *J. Mar. Syst.* **2006**, *60*, 365–380. [[CrossRef](#)]
17. Smagorinsky, J. General circulation experiments with the primitive equations: I. The basic experiment. *Mon. Weather Rev.* **1963**, *91*, 99–164. [[CrossRef](#)]
18. Iwasaki, S.; Isobe, A.; Kako, S.I.; Uchida, K.; Tokai, T. Fate of microplastics and mesoplastics carried by surface currents and wind waves: A numerical model approach in the Sea of Japan. *Mar. Pollut. Bull.* **2017**, *121*, 85–96. [[CrossRef](#)]
19. Kwoun, C.H.; Cho, K.D.; Kim, D.S. A Numerical simulation for the circulation of sea water in the Southern Coastal Waters in Korea. *J. Korean Sci. Mar. Environ. Eng.* **2002**, *5*, 27–40. (In Korean)
20. Egbert, G.D.; Erofeeva, S.Y. Efficient inverse modeling of barotropic ocean tides. *J. Atmos. Ocean Technol.* **2002**, *19*, 183–204. [[CrossRef](#)]
21. Qian, W.; Lee, D.K. Seasonal march of Asian summer monsoon. *Int. J. Climatol.* **2000**, *20*, 1371–1386. [[CrossRef](#)]
22. Rypina, I.I.; Jayne, S.R.; Yoshida, S.; Macdonald, A.M.; Buesseler, K. Drifter-based estimate of the 5 year dispersal of Fukushima-derived radionuclides. *J. Geophys. Res. Oceans* **2014**, *119*, 8177–8193. [[CrossRef](#)]
23. Mao, Y.; Lin, F.; Fang, J.; Fang, J.; Li, J.; Du, M. Bivalve Production in China. In *Goods and Services of Marine Bivalves*; Springer: Cham, Switzerland, 2019; pp. 51–72.
24. Chen, C.L.; Kuo, P.H.; Lee, T.C.; Liu, C.H. Snow lines on shorelines: Solving Styrofoam buoy marine debris from oyster culture in Taiwan. *Ocean Coast. Manag.* **2018**, *165*, 346–355. [[CrossRef](#)]
25. Critchell, K.; Grech, A.; Schlaefer, J.; Andutta, F.P.; Lambrechts, J.; Wolanski, E.; Hamann, M. Modelling the fate of marine debris along a complex shoreline: Lessons from the Great Barrier Reef. *Estuar. Coast. Shelf Sci.* **2015**, *167*, 414–426. [[CrossRef](#)]
26. Turner, A. Foamed polystyrene in the marine environment: Sources, additives, transport, behavior, and impacts. *Environ. Sci. Technol.* **2020**, *54*, 10411–10420. [[CrossRef](#)] [[PubMed](#)]
27. Póvoa, A.A.; de Araújo, F.V.; Skinner, L.F. Macroorganisms fouled in marine anthropogenic litter (rafting) around a tropical bay in the Southwest Atlantic. *Mar. Pollut. Bull.* **2022**, *175*, 113347. [[CrossRef](#)] [[PubMed](#)]
28. Neumann, D.; Callies, U.; Matthies, M. Marine litter ensemble transport simulations in the southern North Sea. *Mar. Pollut. Bull.* **2014**, *86*, 219–228. [[CrossRef](#)] [[PubMed](#)]
29. Mansui, J.; Molcard, A.; Ourmieres, Y. Modelling the transport and accumulation of floating marine debris in the Mediterranean basin. *Mar. Pollut. Bull.* **2015**, *91*, 249–257. [[CrossRef](#)] [[PubMed](#)]
30. Allison, N.L.; Dale, A.; Turrell, W.R.; Aleynik, D.; Narayanaswamy, B.E. Simulating the distribution of beached litter on the northwest coast of Scotland. *Front. Environ. Sci.* **2022**, *10*, 940892. [[CrossRef](#)]
31. Fazey, F.M.; Ryan, P.G. Biofouling on buoyant marine plastics: An experimental study into the effect of size on surface longevity. *Environ. Pollut.* **2016**, *210*, 354–360. [[CrossRef](#)]

Disclaimer/Publisher’s Note: The statements, opinions and data contained in all publications are solely those of the individual author(s) and contributor(s) and not of MDPI and/or the editor(s). MDPI and/or the editor(s) disclaim responsibility for any injury to people or property resulting from any ideas, methods, instructions or products referred to in the content.